Indian Journal of Pure & Applied Physics
Vol. 62, August 2024, pp. 700-711
DOI: 10.56042/ijpap.v62i8.7746

Assessment of Natural Radioactivity and Monitoring of Radiological Hazards in Construction Materials from Kerala, India

Vishnu C V* & Antony Joseph
Department of Physics, University of Calicut, Kerala 673 635, India

Received 2 January 2024; accepted 1 May 2024

Evaluating the natural radioactivity in construction materials is significant, particularly considering the prevailing belief that our homes offer the safest living environments. To investigate this, 38 samples of building materials were collected from highly populated residential areas within the Malappuram district in Kerala, India. The levels of naturally occurring radionuclides (^{226}Ra, ^{232}Th, and ^{40}K) were quantified using a NaI (Tl) detector. Radiological indices, such as radium equivalent, absorbed dose rate, effective dose rate, hazard indices, alpha index, gamma index, and cancer risk, were calculated for the samples. The activity concentrations of ^{226}Ra, ^{232}Th, and ^{40}K ranged from 8.84 ± 0.3 (flooring oxide) to 46.84 ± 2.11Bq/kg (rock samples), 11.84 ± 0.2 (pumice sample) to 130.21 ± 8Bq/kg (granite sample), and 58.63 ± 4 (pumice) to 1024.32 ± 22Bq/kg (granite) with an average of 25.80 ± 4.61, 55.05 ± 6.2, and 392.30 ± 16 Bq/kg. (average ± standard deviation), respectively. As a result, all of these computed parameters fell within safe limits. The examined building materials were found to have a negligible impact on radiation exposure, posing no significant radiation risks to residents. Researchers utilized statistical techniques to understand the interrelationships and similarities among radionuclides and radiological characteristics across samples, including Pearson correlation, principal component analysis, and cluster analysis.

Keywords: Natural radioactivity; Construction materials; Gamma-ray spectrometry; Multivariate statistical techniques

1 Introduction

Naturally occurring radioactive elements, such as those found in the uranium series (derived from ^{238}U), thorium series (derived from ^{232}Th), and actinium series (derived from ^{235}U), play a significant role in contributing to natural radioactivity in the environment. These elements are part of the radioactive decay series. As a result, humans are consistently exposed to ionizing radiation emitted by these naturally occurring radioactive elements (NORM).These radioactive compounds originate from the Earth's crust and can be found in various sources, such as construction materials, water, food, and even human beings. Within this set of sources, natural radon isotopes account for over 50% of the radiation exposure individuals experience from natural sources in the general environment. It is crucial to highlight that these natural radon isotopes have been recognized as the second most significant factor contributing to lung cancer, trailing just behind tobacco smoking[1,2]. Multiple observational studies have revealed a consistent pattern: the likelihood of developing lung cancer rises by 8–12 percent with each 100 Bq/m^3 increase in indoor radon levels. This relationship demonstrates a linear correlation, even when the indoor radon concentration falls below the action level of 200 Bq/m^3 recommended by esteemed organizations such as the International Commission on Radiological Protection (ICRP), the World Health Organization (WHO), and the European Union (EU) for future construction[1,3].

Radiation impacts on the general population, both externally and internally from building materials, are crucial considerations. Internal exposure involves inhaling radon (^{222}Rn), thoron (^{220}Rn), and their decay products, while external exposure relates to gamma radiation-emitting radionuclides. Understanding radionuclide concentrations in construction materials is vital for assessing potential radiological effects on building occupants. Numerous recent studies have investigated the presence of radioactive materials in diverse construction materials and estimated their impact on human health[4,5,14–18,6–13].

Using a NaI (Tl) detector, [15] measured the activity concentrations of ^{226}Ra, ^{232}Th, and ^{40}K in fifty-two samples from eighteen building materials in Erbil city, Kurdistan, Iraq. Radiological indicators evaluated health risks, highlighting potential dangers of granite in

*Corresponding author: (E-mail: venuvishnu24@gmail.com)

poorly ventilated dwellings without windows. However, most other building materials remained within acceptable limits for population safety.

[16]measured the potential radiological risk due to the activity concentrations of primordial radionuclides ^{226}Ra, ^{232}Th, and ^{40}K in commonly used local building materials (sand, clay, kaolin, and gypsum) in Northwestern Nigeria were assessed using NaI (Tl) detector. The acquired results from 28 samples in the study area showed that the health-related risks wereless than international standards[10]. determined radioactivity levels in most commonly used building materials in Kannur district, Kerala, India using well established gamma ray spectrometry employing 5 cm × 5 cm scintillation NaI (Tl) detector. They found that, the contribution to the radiation dose due to the use of these materials for the building construction is insignificant and do not contribute substantial radiation hazards to the occupants.

Typically, the specific activities of ^{238}U, ^{232}Th, and ^{40}K found in unprocessed building materials and their derivatives are influenced by geological and geographical factors, as well as the geochemical characteristics of these materials in specific locations [19].Building materials obtained from the Earth's crust, comprising rocks and soil, can be categorized into four main groups. The first group encompasses structural materials, such as cement, concrete, mortar, clay bricks, pumice bricks, and similar products. The second category comprises materials utilized for insulation and decoration, such as marble, granite, andesite, tuff, gypsum plaster, and similar substances. Lastly, the third category comprises additive raw materials, such as blast furnace slag, fly ash, bauxite, phosphor gypsum, and other substances.

Cement, a composite substance widely used in construction, is composed of various essential components derived from rocks, including limestone, gypsum, clay, and iron ore. On the contrary, ceramic tiles show elevated levels of natural radioactivity compared to other construction materials, mainly attributed to the zircon content in their glaze. Gypsum has been a widely used construction material for an extended period, appreciated for its robustness relative to its thickness and the occurrence of specific trace minerals. M-Sand offers several advantageous features, such as its ability to serve as a filler material and reduce environmental impact. Additionally, M-Sand is advantageous due to its purity, being free from impurities like dust, clay, and silt. This purity prevents any hindrance to the bond between cement paste and aggregates, resulting in reduced water requirements compared to river sand[12].

The primary objective of this research was to evaluate the activity levels of naturally occurring radionuclides, namely ^{226}Ra, ^{232}Th, and ^{40}K, in 38 samples of commonly used construction materials collected from Malappuram city, located in Kerala, India. Gamma-ray spectrometry was employed as the analytical technique for this research. The main objectives were to establish reference data regarding the radioactivity levels in building materials utilized for residential construction in Malappuram province and assess their potential radiological impact. It is essential to evaluate the potential radiological hazards linked to these materials; various parameters were calculated, including radium equivalent activity (Ra_{eq}), indoor gamma absorbed dose rate (D_R), annual effective dose (AED), alpha index (I_α), gamma index (I_γ), external radiation hazard index (H_{ext}), internal radiation hazard index (H_{int}), and excess lifetime cancer risk (ELCR). Additionally, a comparative analysis was conducted, comparing the obtained results with data from construction materials in different countries. Additionally, the radiological parameters underwent a comparison to recommended values by the United Nations Scientific Committee on the Effects of Atomic Radiation (UNSCEAR) and internationally accepted values by the International Commission on Radiological Protection (ICRP). Moreover, basic statistical methods were employed for analysis to gain insights into the statistical characteristics of radionuclide activities found in the samples.

2 Material and Methods

2.1 Material Collection and Preparation

A total of thirty-eight samples, weighing approximately 2–3 kg each, were collected from local suppliers and construction sites in Malappuram district, Kerala, based on their availability. The selected samples represented commonly used construction materials such as cement, white cement, limestone, gypsum, flooring oxides, clay, red bricks, rocks, fly ash, sand, M-sand, marble, tiles, and granite. The sampling locations were chosen to include densely populated residential areas and areas with a high concentration of buildings.

To prepare the samples for analysis, they underwent an initial cleaning and air-drying at room

temperature. Afterwards, the samples were further dried in an oven at 110 °C for 24 hours until a constant dry weight was attained. Following the drying process, the samples were sieved through a 250-μm mesh to ensure uniformity. Subsequently, approximately 300–400 grams of each sample were meticulously stored in airtight plastic containers for a period of 30 days. The sampleswere then hermetically sealed, weighed, and stored in airtight plastic containers(Marinelli containers)of diameter 6.5 cm and height 8.4 cm, standardized to 4π geometry.This step aimed to prevent the release of radiogenic gases, such as radon (^{222}Rn) and thoron (^{220}Rn), and to allow for the establishment of a state of radioactive balance with their respective decay products[20,21]. The samples were then analyzed following standard techniques.

2.2 Activity Concentration

The radioactivity levels in the samples were assessed using a gamma-ray spectrometer equipped with a flat-type Nal (TI) crystal of size 3" x 3". This crystal is used in environmental studies as it has high efficiency, and the operating voltage of the detector is +1000 V. The detector was paired with a multichannel analyzer and calibrated using standard sources of RG-U, RG-Th, and RG-K obtained from the International Atomic Energy Agency in Vienna. To measure the radioactivity of the samples using radiometric methods, the counting time for detecting emitted photons was established at 105 seconds (equivalent to 28 hours). Energy calibration was conducted using multi-gamma-ray standard sources—137Cs, 60Co, 54Mn, 152Eu, and 22Na—which emit gamma radiation in the range of 356–1333 keV and are traceable to international standards. To minimize background radiation counts, the detector was enclosed in graded lead shielding, analyzing the ^{137}Cs (661 keV) peak; the full-width half-maximum was determined to be 60.78 keV. With an acquisition time of 80,000 s and sufficient statistical data, the gamma-ray spectrum of the samples was collected and analyzed using GSPEC software. The counts obtained from the analysis were then used to calculate the concentration of radionuclides, specifically ^{226}Ra, ^{232}Th, and ^{40}K, present in the samples. The concentration of ^{226}Ra was calculated based on the 1764 keV gamma peaks of ^{214}Bi. For the determination of ^{232}Th, the gamma transition of ^{208}Tl at 2614 keV was utilized. Similarly, the concentration of the radionuclide ^{40}K in the various samples was determined using the 1460.8 keV gamma peak emitted by ^{40}K itself[22].

Simultaneous equations were utilized to analyze the spectrum and compute the concentrations of ^{226}Ra, ^{232}Th, and ^{40}K radionuclides [10,23]:

$$C_1 = T_{2.16} \quad \ldots (1)$$

$$C_2 = T_{1.76} - F_1 \quad \ldots (2)$$

$$C_3 = T_{1.46} - F_2C_1 - F_3C_2 \quad \ldots (3)$$

where C_1, C_2, and C_3 are the Compton's corrected and background-subtracted counts of the photopeaks ^{232}Th, ^{226}Ra, and ^{40}K, respectively, wherein $T_{2.61}$, $T_{1.76}$, and $T_{1.46}$ are the full integration counts for photo peaks of ^{208}Tl, ^{214}Bi, and^{40}K. The factors contributing to Compton are F_1, F_2, andF_3. The ^{226}Ra, ^{232}Th, and ^{40}K activity concentrations were evaluated using Eq. (4) [10,22]:

$$AC = (CC \pm SD) \times \frac{100}{E} \times \frac{100}{A} \times \frac{100}{W} Bq/kg \quad \ldots (4)$$

where CC is the Compton corrected net count, SD is standard deviation, E is the photopeak efficiency of the detector, A is the abundance of the characteristic gamma ray, W is the mass of the samples in grams[20].

2.3 Hazard indices and dose parameters

Table 1 shows radiological hazard parameters associated with natural radioactivity. The main focus of the present study was to assess the radiation risks associated with the building material samples by evaluating various radiological parameters. These parameters included radium equivalent activity (Ra_{eq}),

Table 1 — Radiological hazards associated with natural radioactivity.

Radiological hazards	Equations used for calculation	Units	Equation Number
Radium equivalent activity	$Ra_{eq} = A_{Ra} + 1.43A_{Th} + 0.077A_K$	($Bqkg^{-1}$)	(5)
Absorbed dose rate	$D_R = 0.92A_{Ra} + 1.1A_{Th} + 0.08A_K$	($nGyh^{-1}$)	(6)
Annual effective dose equivalent	$AED_{indoor} = D_R\ (nGyh^{-1}) \times 8760\ h \times 0.8 \times 0.7\ SvGy^{-1} \times 10^{-6}$	(μSvy^{-1})	(7)
External hazard index	$H_{int} = A_{Ra}/370 + A_{Th}/259 + A_K/4810$	-	(8)
Internal hazard index	$H_{ext} = A_{Ra}/185 + A_{Th}/259 + A_K/4810$	-	(9)
Gamma index	$I_\gamma = A_{Ra}/300 + A_{Th}/200 + A_K/3000$	-	(10)
Alpha Index	$I_\alpha = A_{Ra}/200$	-	(11)
Excess lifetime cancer risk	$ELCR_{indoor} = AED_{indoor} \times DL \times RF$	10^{-3}	(12)

gamma absorbed dose rate (D_R), annual effective dose equivalent (AED), excess lifetime cancer risk (ELCR), internal hazard index (H_{int}), external hazard index (H_{ext}), gamma index (Iγ), and alpha index (I_α).These parameters were utilized to quantify the potential risk by determining the amount of radiation emitted by the primordial radionuclides, namely ^{226}Ra, ^{232}Th, and ^{40}K, present in the building materials[13,24,25].

2.4 Multivariate Statistical Analysis

In this study, multivariate statistical analysis techniques, including the Pearson correlation coefficient, cluster analysis, and principal component analysis (PCA), were utilized to investigate the interrelationships and connections among the variables under examination. The primary objective was to investigate the influence of the identified radiological features and the distribution of natural radionuclides within the samples. Mainly, the Pearson correlation coefficient was used to measure the strength of the associations between the variables of interest. Cluster analysis, on the other hand, was employed to represent the degree of associations among the variables visually. PCA, a commonly used method, was applied to summarize the patterns among the variables in the dataset. To prepare the data for PCA analysis, the Varimax normalization approach was used. PCA is widely utilized because it allows for data compression by reducing the number of dimensions while retaining important information, particularly when correlations are observed. The statistical analysis of the collected data was conducted using IBM SPSS Statistics V21.0, which provided the necessary tools and functionalities for the required analyses.

3 Results and Discussion

3.1 Activity Measurement

Figure 1 shows the gamma energy spectrum of rock sample under this study. Table 2 presents the activity concentrations of ^{226}Ra, ^{232}Th, and ^{40}K in the samples, as determined from the observed spectra, which included energies corresponding to daughters of long-lived radioactive materials and direct energies.

The activity concentration of ^{226}Ra ranged from 8.62±2 to 46.84±8.6 Bqkg^{-1}, with a mean value of 27 ±5 Bqkg^{-1}. The highest concentration of ^{226}Ra was found in the rock sample, while the lowest was in the flooring oxide sample. For ^{232}Th, the activity concentrations in the measured samples varied from 11.84±3 Bqkg^{-1} (in the pumice sample) to 130.21±11 Bqkg^{-1} (in the marble sample), with a mean value of 55.16±4 Bqkg^{-1}.The activity concentrations of ^{40}K were also measured, ranging from 58.63±10 Bqkg^{-1} (in the pumice sample) to 1024.32±44 Bqkg^{-1} (in the granite sample). The average activity concentration of ^{40}K was found to be 384.43±21 Bqkg^{-1}.These concentrations were compared with values found in the literature, as well as the recommended limits by UNSCEAR and ICRP 60[1,26]. Among the different samples evaluated, only the clay powder and sand exhibited ^{226}Ra concentrations that exceeded the upper limit suggested by the literature. Higher activity levels of ^{226}Ra, ^{232}Th, and ^{40}K were detected in various construction materials, including rocks, tiles, cement, sands, and granite. However, apart from the pumice and flooring oxide samples, these concentrations did not significantly exceed the global average values.

According to Table 2, the primary sources of gamma radiation in the construction materials analyzed for this study are ^{232}Th and ^{40}K. The activity of ^{226}Ra, ^{232}Th, and ^{40}K radionuclides are displayed in Fig. 2 for easy comparison.

The average activity concentrations of natural occurring radioactive materials (NORM) in the analyzed building materials were compared to the global average values of 50 Bqkg^{-1} for ^{226}Ra, 50 Bqkg^{-1} for ^{232}Th, and 500 Bqkg^{-1} for ^{40}K. It was observed that the average concentration of ^{232}Th activity slightly exceeded the global average.

3.2 Radiological Risk Parameters

Table 3 illustrates the Radiological parameters of the samples. The distribution of ^{226}Ra, ^{232}Th, and ^{40}K

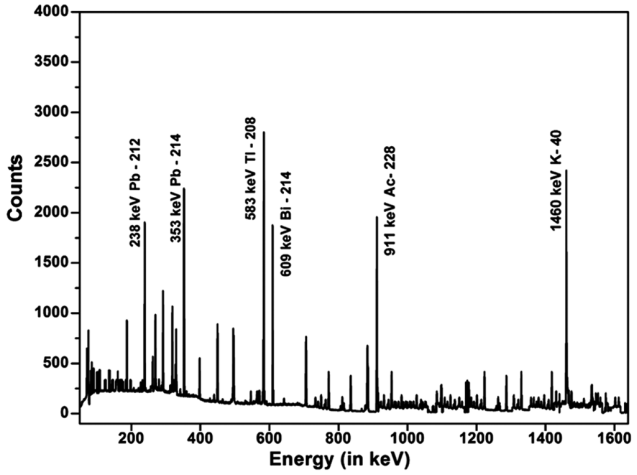

Fig. 1 — The gamma energy spectrum of rock sample under this study

Table 2 — Activity concentration of ^{226}Ra, ^{232}Th and ^{40}K in building materials.

Sample Name	No		Activity Concentration (Bqkg^{-1})		
			^{226}Ra	^{232}Th	^{40}K
Cement	3	Range	25.68-34.26	35.26-47.35	82.68-102.25
		Average	29.43	42.98	92.43
White cement	2	Range	18.32-35.23	32.36-54.41	92.43-141.21
		Average	26.78	43.39	138.81
Limestone	3	Range	12.68-18.47	28.69-34.36	138.96-181.24
		Average	15.50	31.95	155.52
Flooring Oxides	3	Range	8.84-10.25	23.68-27.32	68.24-74.13
		Average	9.42	25.45	70.88
Gypsum	2	Range	18.54-35.85	38.68-59.34	85.41-128.68
		Average	25.08	46.47	103.07
Pumice	2	Range	20.52-22.48	11.84-16.21	58.63-70.28
		Average	21.50	14.03	64.46
Fly ash Powder	2	Range	15.84-18.95	42.35-56.43	98.36-112.46
		Average	17.39	46.79	105.41
Red Bricks	2	Range	22.81-34.22	55.14-65.18	421.32-650.25
		Average	28.86	60.16	535.78
Clay	3	Range	18.68-24.44	32.25-61.42	256.25-512.48
		Average	21.86	45.35	364.12
Marble	3	Range	19.58-36.84	81.25-130.21	480.35-625.48
		Average	26.91	104.99	582.38
Granite	3	Range	23.28-44.28	42.68-102.28	841.54-1024.32
		Average	33.43	74.30	941.09
Tiles	3	Range	28.38-41.12	29.36-86.84	326.54-615.28
		Average	34.60	65.16	454.07
Rock powder	3	Range	34.25-46.84	74.28-91.54	684.38-814.26
		Average	39.84	81.82	751.09
M-sand	2	Range	21.25-24.58	33.45-36.74	762.84-689.67
		Average	22.92	35.09	726.40
Sand	2	Range	24.47-33.48	83.15-105.68	648.64-812.38
		Average	28.98	93.92	730.51

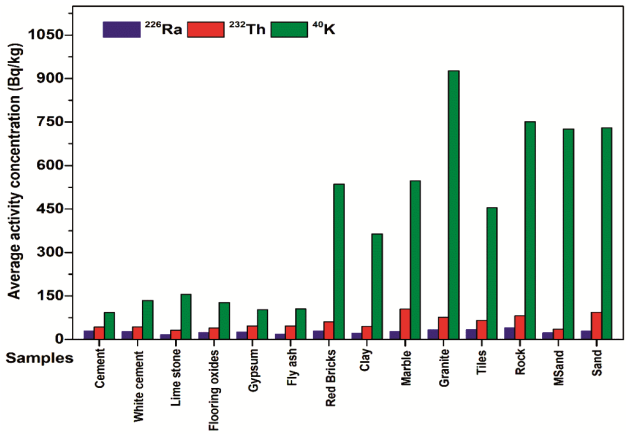

Fig. 2 — Activity of ^{226}Ra,^{232}Th and ^{40}K in different building materials

activity in the environmental samples was found to be non-uniform. To assess the overall activity and radioactive risk associated with building materials containing ^{226}Ra, ^{232}Th, and ^{40}K, the radium equivalent activity (Ra_{eq}) was calculated using Eq. 5.

Table 3 displays the average radium equivalent activity and absorbed gamma dose rates for each type of construction material. The distribution of natural radionuclides in all the samples demonstrated a lack of uniformity.The degree of uniformity in terms of radiation exposure can be characterized using the concept of radium equivalent activity (Ra_{eq}). The Ra_{eq} values ranged from 44.82 to 269.41 Bqkg^{-1}, with an average of 134.08 Bqkg^{-1}. The average Ra_{eq} value was significantly lower than the permissible limit of 370 Bqkg^{-1}. Therefore, the calculated mean Ra_{eq} value, which is only about half of the maximum allowable value, does not raise any concerns regarding radioactivity when these materials are used in construction. Fig. 3 illustrates the relationship between Raeq and absorbed dose rate (D_R) for various types of construction materials. Evaluating the radiation exposure to gamma radiation relies heavily on determining the dose rate (D_R), which is considered the most crucial aspect. The dose rate indicates the amount of energy transferred to matter per unit mass by ionizing radiation.

The average absorbed gamma dose rates (D_R) varied from 39.33 to 235.19 nGy/h, with an average

Table 3 — Radiological risk parameters of the samples.

Sample	Radiological parameters							
	Ra_{eq} ($Bqkg^{-1}$)	D_R ($nGyh^{-1}$)	H_{ext}	H_{int}	I_α	I_γ	AED (μSvy^{-1})	ELCR (10^{-3})
Cement	98.02	81.76	0.26	0.34	0.15	0.69	100.27	0.35
White cement	99.21	83.15	0.27	0.34	0.13	0.70	101.98	0.36
Limestone	73.17	61.85	0.20	0.24	0.08	0.53	75.86	0.27
Flooring Oxides	90.13	75.59	0.24	0.31	0.12	0.64	92.70	0.32
Gypsum	99.46	82.43	0.27	0.34	0.13	0.70	101.09	0.35
Fly ash Powder	92.43	75.91	0.25	0.30	0.09	0.65	93.10	0.33
Red Bricks	155.80	135.27	0.42	0.50	0.14	1.15	165.90	0.58
Clay	114.75	99.13	0.31	0.37	0.11	0.84	121.57	0.43
Marble	219.21	184.05	0.59	0.66	0.13	1.59	225.72	0.79
Granite	215.33	189.94	0.58	0.67	0.17	1.61	232.94	0.82
Tiles	162.19	139.32	0.44	0.53	0.17	1.18	170.86	0.60
Rock powders	214.69	186.75	0.58	0.69	0.20	1.58	229.03	0.80
MSand	129.02	117.79	0.35	0.41	0.11	0.99	144.45	0.51
Sand	219.52	188.40	0.59	0.67	0.14	1.62	231.06	0.81
Total average	134.08	114.99	0.36	0.43	0.13	0.98	141.12	0.43
World average	370	84	1	1	1	1	70	1.16

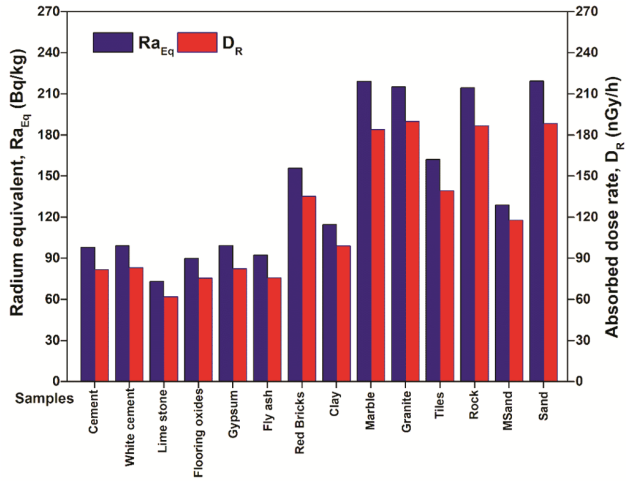

Fig. 3 — Radium equivalent activity and dose rate of different construction materials

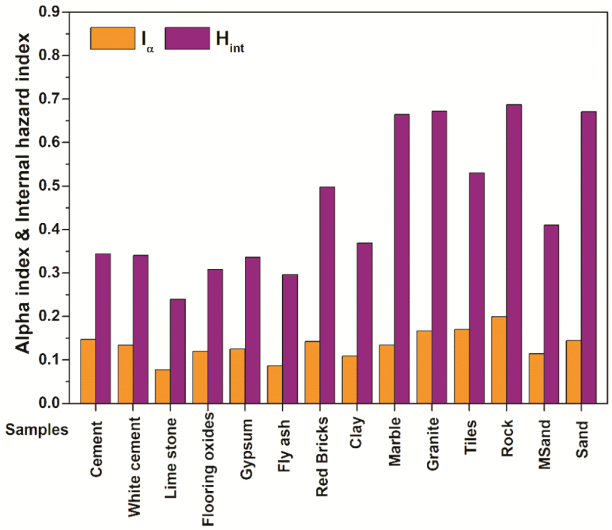

Fig. 4 — Variation of I_α and H_{int} of the building material samples

value of 114.99 nGy/h. For most of the selected building materials in this study, the average D_R values were higher than the world population weighted average indoor absorbed gamma dose rate of 84 nGy/h[1,27]. Table 3 provides the radiological parameters including hazard indices (H_{ext} and H_{int}), Alpha index (I_α), Gamma index (I_γ), Excess lifetime cancer risk (ELCR), and Annual effective dose equivalent (AED). The calculated Hext values ranged from 0.12 to 0.73, with a mean value of 0.36, which is below the criterion value of 1. Fig. 4 & 5 illustrate the variability of the alpha and gamma indices.

The H_{int} values obtained were all below 1, indicating that the internal hazard posed by the analyzed building material samples is below the criterion value. The H_{int} values ranged from 0.15 to 0.85, with an average of 0.43. These findings

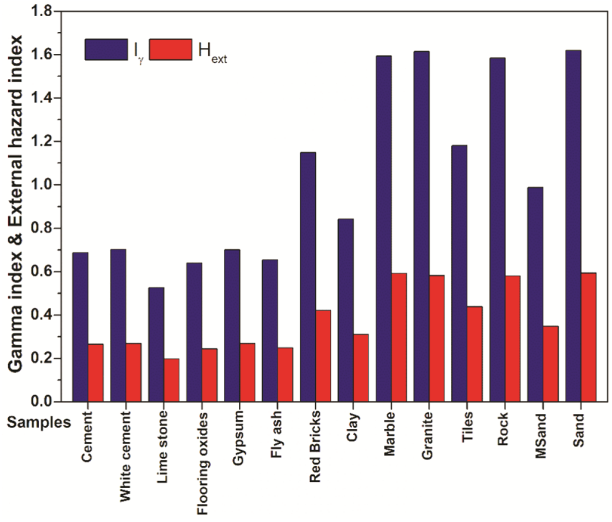

Fig. 5 — Variation of I_γ and H_{Ext} of the building material samples

demonstrate that the external and internal gamma radiation does not present any radiological hazards when these materials are used in building construction. The calculated I_γ values in the studied samples are less than the recommended limit of 1. As a result, radon inhalation from the analyzed region's samples is insignificant. As a result, using these materials for building is risk-free. The building material samples exhibit an alpha index ranging from 0.04 to 0.23, with a mean value of 0.13. Additionally, the estimated gamma index for these samples ranges from 0.32 to 2.0, with a mean value of 0.98. As a result, the annual effective dose conveyed by these building materials remains below the annual effective dose limit of 1 mSv per year.

Figures 6 & 7 show the average value of AED and ELCR of the building material samples. The

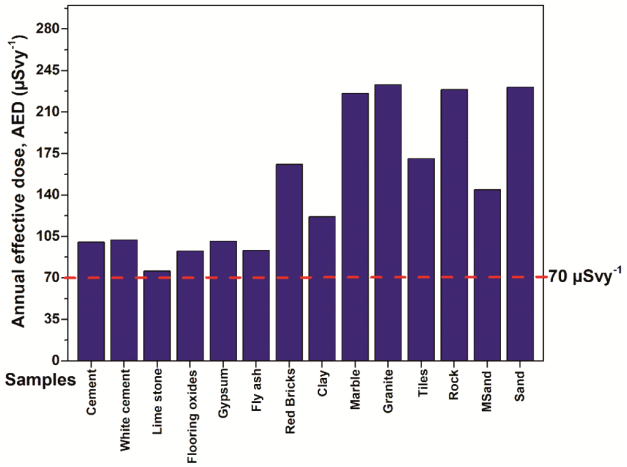

Fig. 6 — Average value of AED of the building material samples

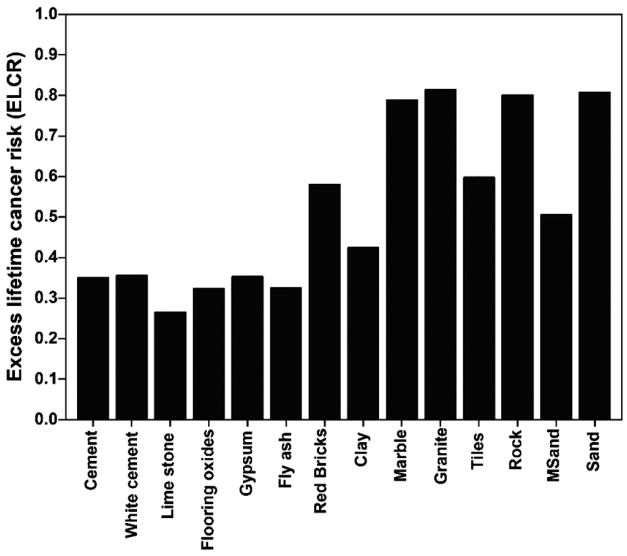

Fig. 7 — Average value of ELCR of the building material samples

estimated indoor annual effective dose rate values ranged from 48.26μSvy^{-1} (Pumice) to 288.64μSvy^{-1} (Granite) with a mean value of 141.12μSvy^{-1}.

The average indoor annual effective dose was higher than the world average value of 70μSvy[11,19]. The excess lifetime cancer risk (ELCR) values obtained show that lower value 0.17×10^{-3} is corresponding to flooring oxide sample, higher value (1.01×10^{-3}) is corresponding to granite sample and the with mean value of 0.49×10^{-3}. The mean value is lower than the world average (1.16×10^{-3}).

Table 4 provides a comparison between the findings of this study and data reported in the literature from various regions around the world. The

Table 4 — Comparison between the mean activity concentrations of the constructing materials used in the present study and other parts of the world.

Materials	Countries	Radioactivity (Bqkg^{-1})			
		^{226}Ra	^{232}Th	^{40}K	References
Cement	Bangladesh	61	65	952	[28]
	Malaysia	29	31	205	[29]
	Nigeria	21	16	147	[30]
	Iraq	28.2	14.2	303.4	[15]
	India	37	34	188	[19]
	India	28.9	14.81	31.67	[10]
	India	29.43	42.99	92.43	Present work
Sand	Bangladesh	54	77	982	[28]
	Iran	24	22	362	[13]
	Iran	8.69	3.30	75.78	[14]
	Malaysia	43	45	451	[29]
	Nigeria	18	59	236	[30]
	Iraq	15	13	370.6	[15]
	India	11	130	297	[19]
	India	28.98	93.92	730.51	Present work
Gypsum	Bangladesh	254.5	21.4	120.8	[31]
	Iran	12	14	116	[13]
	Nigeria	54.4	27.9	242.4	[16]
	Iraq	3.2	3.3	29.4	[15]
	India	25.08	46.47	103.07	Present work
Marble	Egypt	41	49	317	[31]
	Iran	7	7	917	[13]
	Turkey	30	58	297	[32]
	Iraq	25	4.4	56.1	[15]
	India	9.25	61.63	1366.85	[33]
	India	26.91	104.99	547.55	Present work
Clay	Australia	41	89	681	[19]
	Egypt	33	68	130	[31]
	China	41	52	717	[19]
	Malaysia	241	51	7541	[34]
	Nigeria	54.4	27.4	242.4	[16]
	India	21.86	45.35	364.12	Present work
Granite	Nigeria	74	100	1098	[30]
	Iran	38	47	917	[13]
	China	356	318	1637	[35]
	Iraq	109.4	62.7	836.5	[15]
	India	33.43	77.27	927.37	Present work

mean activity concentrations of radionuclides exhibit variation depending on the country and the source of the materials. When comparing the mean activity concentrations of cement, marble, clay, sand, granite, and gypsum samples in this study with literature values, differences become apparent. The distribution of radium, thorium, and potassium in soil or rocks, which serve as the origins of building materials, is non-uniform and can exhibit variations over short distances.

The recorded values of radium and thorium in soil represent the average radioactivity of a particular area, considering the varying half-lives of these elements. This characteristic also impacts the production of radon, thoron, and their gamma-emitting decay products throughout the lifespan of a building, which can remain relatively stable.

The activity concentration ranges of ^{226}Ra, ^{232}Th, and ^{40}K in the sand samples recorded in this study are like values reported in Nigeria, China, and India. The reported concentrations of radionuclides in sand vary nationally, ranging from 18.0 Bq/kg in Punjab to 445.8 Bq/kg in Kollam for ^{226}Ra, 8.0 Bq/kg in Northern Rajasthan to 2022.0 Bq/kg in Kollam for ^{232}Th, and 78.3 Bq/kg in Kaiga to 1894.0 Bq/kg in Northern Rajasthan for ^{40}K. In comparison with nationwide data, the concentrations of ^{226}Ra and ^{232}Th in the study area fall within the medium range[5,36–38]. Additionally, the results for cement samples match those previously measured in Nigeria. The activity concentrations of these radionuclides in gypsum and granite samples are also comparable to findings from other studies conducted in China.

3.3 Statistical Analysis of the Data

The research investigated and outlined the distribution characteristics of naturally occurring radioactive materials (NORM) in construction materials, with a specific focus on three aspects: concentration trend, degree of dispersion, and shape of the distribution function. Basic statistical measures were employed to describe the properties of the radionuclides, encompassing average activity concentration, minimum and maximum values, standard deviation, kurtosis, variance, and skewness. The statistical attributes of the building materials' data are summarized in Table 5.

Typically, when the standard deviation exceeds the mean value, it indicates a lack of uniformity, while a standard deviation lower than the mean suggests a higher level of consistency. In this study, the standard deviation values for ^{226}Ra, ^{232}Th, and ^{40}K are lower than their respective mean values, indicating a high degree of uniformity and consistency among the samples. Skewness data for natural radionuclides provides valuable insights into the degree of asymmetry in the distribution around their mean in the realm of probability theory and statistics[39,40]. Skewness is a statistical measure utilized to assess the asymmetry of a probability distribution of a real-valued random variable. Analyzing skewness offers various advantages. Numerous models assume a normal distribution, where the data are symmetrically distributed around the mean. A skewness value of zero signifies a perfectly symmetric normal distribution. However, in real-world scenarios, data points may deviate from perfect symmetry. By examining the skewness of a dataset, we can determine whether deviations from the mean are more likely to be positive or negative. In the present study, the skewness values for ^{226}Ra, ^{232}Th, and ^{40}K were found to be 0.24, 0.74, and 0.44, respectively. Positive skewness values imply that the distribution of radionuclides is asymmetrical, with the tail of the distribution extending towards higher positive values. The relatively small skewness values observed indicate that the distributions exhibit some degree of asymmetry in their characteristics[19,41].

Kurtosis is a statistical measure used to assess the level of peakedness in the probability distribution of a random variable with real values. It provides a quantitative assessment of how much the distribution deviates from a flat or normal distribution shape. It indicates whether a distribution is more peaked or flatter than the normal distribution. A higher kurtosis value suggests that a greater proportion of the variation in the data is attributed to extreme deviations rather than frequent moderate deviations[8]. The observed negative kurtosis values indicate that the activity concentration distributions are relatively flat. Specifically, the kurtosis values for ^{226}Ra, ^{232}Th, and ^{40}K are -0.53, -0.27, and -1.27, respectively. The frequency distributions of the radionuclides in the 38

Table 5 — Statistical parameters of the activity concentration ($Bqkg^{-1}$) in samples.

Parameters	^{226}Ra	^{232}Th	^{40}K
Minimum	8.84	11.84	58.63
Maximum	46.84	130.21	1024.32
Mean	25.80	55.05	392.30
Std.dev.	9.62	28.88	303.16
Variance	92.48	834.27	91907.61
Skewness	0.24	0.74	0.44
Kurtosis	-0.53	-0.27	-1.27

samples were examined, and the corresponding histograms are displayed in Fig. 8. The histogram for 226Ra illustrates a normal distribution characterized by a bell-shaped curve. On the other hand, the histograms for 232Th and 40K exhibit some degree of multi-modality, indicating the presence of multiple peaks or modes in their distributions. (Raghu *et al*., 2017; Ravisankar *et al*., 2014). This multimodal property of radioactive elements reveals the variety of mineral composition in the samples.

3.3.1 Pearson's correlation coefficient analysis

The concentrations of individual radionuclides in construction materials can be affected by various factors, encompassing: (1) the geological composition of the source rocks, (2) the mineral content, and (3) the chemical behavior of the radionuclides[42]. Table 6 displays the Pearson correlation coefficients for all the investigated radioactive factors in construction materials from the Malappuram district. When calculating the error-free correlation coefficient (R), the value lies within the range of -1 to 1. A Pearson correlation coefficient of exactly 1.0 indicates a highly robust positive relationship between the two variables, signifying that an increase in one variable is consistently associated with a positive increase in the second variable. Conversely, a value of -1.0 indicates that the variables move in opposite directions, meaning that an increase in one variable is consistently linked to a decrease in the other variable (Oladejo *et al*., 2020). When the correlation coefficient R is equal to 0, it indicates no relationship between the two variables. Strong correlation is defined as $R > 0.75$, moderate correlation as $0.50 \leq R \leq 0.75$, and poor correlation as $0.36 \leq R \leq 0.5$. In this study, a strong positive correlation coefficient ($R < 0.82$) is observed between ^{226}Ra and all other variables, suggesting that the ^{226}Ra activity concentration in the samples significantly influences all other variables. A moderate correlation ($0.62 \leq R \leq 0.75$) is observed between the activity concentrations of ^{232}Th and ^{40}K with all other variables. On the contrary, the correlations between any two combinations of ^{226}Ra, ^{232}Th, and ^{40}K nuclides are very weak. The alpha index shows a very strong correlation with ^{226}Ra and weak correlations with ^{232}Th and ^{40}K. This correlation implies that the concentrations of ^{226}Ra and ^{40}K are the main contributors to the radiological hazards posed by these building materials[41].

3.3.2 Principal Component Analysis (PCA)

PCA, an extensively employed multivariate statistical technique in environmental studies, is a

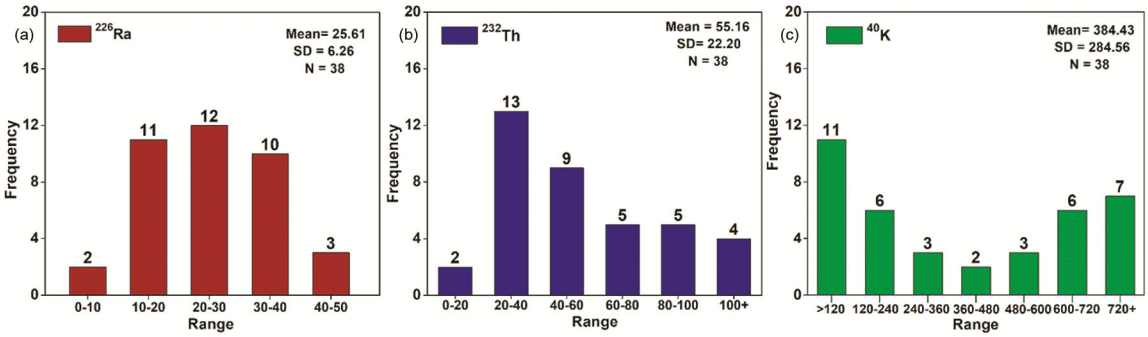

Fig. 8 — The frequency distribution of the activity concentration of ^{226}Ra, ^{232}Th and ^{40}K

Table 6 — Pearson correlation of radioactive parameters.

Variables	^{226}Ra	^{232}Th	^{40}K	Ra_{eq}	D_R	I_α	I_γ	AEDE	ELCR	H_{ext}	H_{int}
^{226}Ra	1.000										
^{232}Th	0.629	1.000									
^{40}K	0.729	0.582	1.000								
Ra_{eq}	0.866	0.787	0.702	1.000							
D_R	0.879	0.748	0.715	0.879	1.000						
I_α	1.000	0.449	0.541	0.866	0.999	1.000					
I_γ	0.854	0.779	0.724	0.999	0.999	0.879	1.000				
AEDE	0.879	0.788	0.655	0.998	0.998	0.879	0.980	1.000			
ELCR	0.879	0.748	0.715	0.988	0.998	0.879	0.999	0.997	1.000		
H_{ext}	0.866	0.786	0.713	0.990	0.998	0.866	0.999	0.998	0.988	1.000	
H_{int}	0.939	0.795	0.675	0.985	0.988	0.939	0.980	0.988	0.988	0.985	1.000

favoured tool for data reduction and extracting independent components known as principal components. It enables the evaluation of correlations among observable variables. This study contributes novel fundamental components that enhance the precision and quantitative interpretation of geochemical data[43]. In this study, PCA was conducted on the dataset consisting of 11 variables. Table 7 gives the results of PCA with varimax rotation. Varimax rotation with Kaiser Normalization was employed to identify the variables, and the graphical representation of the Principal Component Analysis (PCA) results is displayed in Fig. 8. The correlation matrix was used to extract eigen values and eigenvectors, which helped identify the number of significant factors and the percentage of variance explained by each of these factors[44].

The findings demonstrate that these three factors account for over 97.98% of the total variance. Typically, an ordination result is considered satisfactory if it reaches 75% or higher[3]. Upon analyzing the rotated space of Component 1, Component 2, and Component 3 (as depicted in Fig. 9), it becomes evident that the first factor contributes to 45.76% of the total variance. This factor is distinguished by a high positive loading of ^{226}Ra concentrations[45]. The second factor explains 30.89% of the total variance and is primarily associated with a positive loading of ^{232}Th. Lastly, the third factor accounts for 21.35% of the total variance and is linked to a positive loading of ^{40}K. Overall, the factor analysis reveals that ^{226}Ra and ^{232}Th exert a dominant influence on the observed radioactivity levels in all the building materials.

3.3.3 Hierarchical Cluster Analysis (HCA)

Given the complexity resulting from many variables in correlation studies, hierarchical cluster analysis (HCA) provides a valuable approach to better understand and visually represent the correlations among all radioactive variables. Hierarchical Cluster Analysis (HCA) is an approach to data classification that employs a set of multivariate algorithms to detect meaningful clusters within the data[39]. While there are various clustering methods available, hierarchical clustering is the most utilized one. This clustering technique groups similar objects together, forming distinct classes. Hierarchical clustering prioritizes categorizing observations with the highest similarity, followed by grouping the next most similar observations[46].

The classification process is performed iteratively until all observations are assigned to their respective categories. As a result of this process, a dendrogram is created, illustrating the levels of similarity at which observations are combined[45]. As shown in Fig. 10, the

Table 7 — Rotated factor loading of the variables.

Variables	Component 1	Component 2	Component 3
^{226}Ra	0.941	0.238	0.241
^{232}Th	0.503	0.972	0.218
^{40}K	0.486	0.369	0.938
Ra_{eq}	0.852	0.621	0.435
D_R	0.869	0.573	0.474
AEDE	0.869	0.573	0.474
ELCR	0.778	0.628	0.474
I_α	0.941	0.273	0.241
I_γ	0.844	0.611	0.477
H_{ext}	0.846	0.619	0.436
H_{int}	0.837	0.508	0.381
% Variance	45.76	30.89	21.35

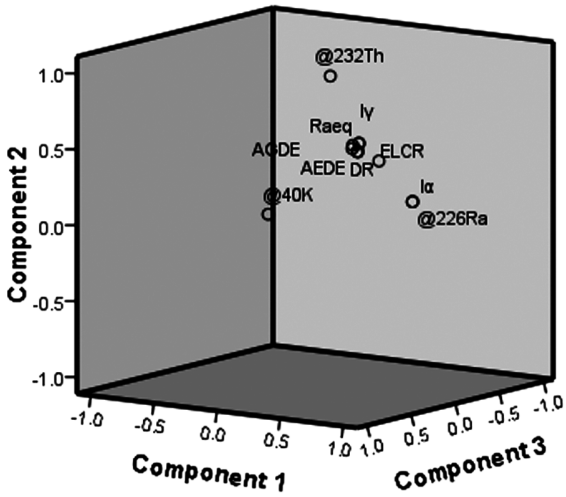

Fig. 9 — Graphical representation of components

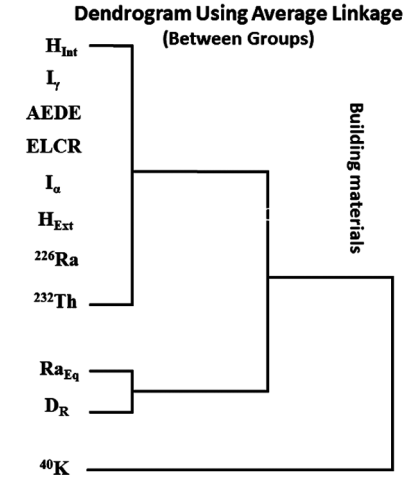

Fig. 10 — Dendrogram shows cluster formation of variables

generated dendrogram illustrates the clustering of variables in the present study. The outcomes obtained from the cluster analysis align with the findings of the correlation analysis. Cluster analysis was utilized to evaluate the degrees of similarity among the radioactivity levels and the derived radiological hazard parameters. The dendrogram vividly illustrates the intercorrelations between ^{226}Ra and ^{232}Th activity concentrations on one side, and all other radiological hazard metrics on the other side.

Moreover, the dendrogram indicates that ^{40}K exhibits a weak association with other metrics, implying that potassium's activity concentration does not significantly contribute to the radioactivity of construction materials. The results obtained from the dendrogram closely correspond with the outcomes of the correlation and factor analysis.

4 Conclusion

The study examined the natural radionuclide content and radiological parameters of commonly utilized construction materials in the Malappuram district of Kerala, India. The parameters examined included radium equivalent activity (Ra_{eq}), indoor gamma absorbed dose rate (D_R), annual effective dose equivalent (AEDE), alpha index (Iα), gamma index (I_γ), external radiation hazard index (Hext), internal radiation hazard index (Hint), and excess lifetime cancer risk (ELCR). Results are summarized below.

1. The activity concentrations of ^{226}Ra, ^{232}Th, and ^{40}K ranged from 8.84 ± 0.3 (flooring oxide) to 46.84 ± 2.11 Bq/kg (rock samples), 11.84 ± 0.2 (pumice sample) to 130.21 ± 8 Bq/kg (granite sample), and 58.63 ± 4 (pumice) to 1024.32 ± 22 Bq/kg (granite) with an average of 25.80 ± 4.61, 55.05 ± 6.2, and 392.30 ± 16 Bq/kg. (average ± standard deviation), respectively.
2. The Ra_{eq} values ranged from 44.82 to 269.41 Bqkg^{-1}, with an average of 134.08 Bqkg^{-1}. The average Ra_{eq} value was significantly lower than the permissible limit of 370 Bqkg^{-1}.
3. The average absorbed gamma dose rates (D_R) varied from 39.33 to 235.19 nGy/h, with an average value of 114.99 nGy/h. For most of the selected building materials in this study, the average D_R values were higher than the world population weighted average indoor absorbed gamma dose rate of 84 nGy/h[1,27].
4. The estimated indoor annual effective dose rate values ranged from 48.26 μSvy^{-1} (Pumice) to 288.64 μSvy^{-1} (Granite) with a mean value of 141.12 μSvy^{-1}.
5. The excess lifetime cancer risk (ELCR) values obtained show that lower value 0.17×10^{-3} is corresponding to flooring oxide sample, higher value (1.01×10^{-3}) is corresponding to granite sample and the with mean value of 0.49×10^{-3}. The mean value is lower than the world average (1.16×10^{-3}).
6. Factor analysis reveals that ^{226}Ra and ^{232}Th exert a dominant influence on the observed radioactivity levels in all the building materials.

The study's results indicated that these parameters' values were within the recommended safety limits. This indicates that the building materials examined do not present a significant radiation hazard, thereby ensuring their safety for use in constructing residences for the inhabitants of the area. The statistical analysis revealed that the average values of rock and granite samples were slightly higher than the global average values. The analysis also showed that rock, sand, granite, and tile materials had higher concentrations of ^{226}Ra, ^{232}Th, and ^{40}K compared to cement and other flooring samples. Among these radionuclides, ^{226}Ra and ^{232}Th were found to be the primary contributors to the overall radioactivity levels, while ^{40}K had a relatively minor impact. To explore the relationships and correlations among the different samples in a more systematic manner, using multivariate statistical techniques, specifically including the Pearson correlation coefficient, cluster analysis, and principal component analysis. These techniques provided valuable insights into the similarities and associations between the samples. In summary, the study's findings indicated that the frequently used construction materials analyzed in the Malappuram district do not pose any notable radiation hazard. As a result, their use in construction is deemed safe, with no radiological threat to the occupants of the buildings.

Acknowledgements

The authors express their gratitude to the Central Sophisticated Instrumentation Facility (CSIF) at the University of Calicut, Kerala, for granting access to elemental analysis facilities.

Author contribution

The study's inception and design were collaboratively developed with input from all the authors. Vishnu C V took charge of material gathering, data collection,

analysis, and manuscript writing. Dr. Antony Joseph provided valuable supervision and offered constructive feedback on earlier drafts of the work.

Reference

1 UNSCEAR, *Sources, Effects and Risks of Ionizing Radiation*, 120 (2008). https://doi.org/10.2307/3577647.

2 WHO, *WHO Handbook on Indoor Radon: A Public Health Perspective. Geneva: World Health Organization,* 2009.

3 Mann N, Kumar A, Kumar S & Chauhan R P, Indoor and Built, Measurement of Radium , Thorium , Potassium and Associated Hazard Indices from the Soil Samples Collected from Northern India, *Sage J*, 27 (2017) 1.

4 Ding X, Lu X, Zhao C, Yang G & Li N, *Radiat Prot Dosimetry*, 155 (2013) 374.

5 Devanesan E, Chandramohan J, Senthilkumar G, Harikrishnan N, Gandhi S M, Kolekar S S & Ravisankar R, *Shengtai Xuebao/ Acta Ecol Sin*, 40 (2020) 353. https://doi.org/10.1016/j.chnaes.2019.06.001.

6 Kumar M, Sahoo B K, Kumar R & Sharma N, *Radiat Prot Environ*, 43 (2020) 31.

7 Senthilkumar G, Ravisankar R, Vanasundari K, Vijayalakshmi I, Vijayagopal P & Jose M T, *Radiat Phys Chem,* 88 (2013) 45.

8 Hamideen M S, *Int J Environ Anal Chem,* 102 (2020) 380.

9 Ndour O, Thiandoume C, Traore A, Cagnat X, Diouf P M, Ndeye M, Ndao A S & Tidjani A, *SN Appl Sci,* 2 (2020) 1.

10 Mahamood K N & Narayana C S K Y, *J Radioanal Nucl Chem,* 322 (2019) 105.

11 Balakrishnan D, *Int J Fundam Phys Sci,* 2 (2012) 41.

12 Rajalakshmi V T A & Jananee A C B, *J Radioanal Nucl Chem*, 324 (2020) 1059.

13 Imani M, Adelikhah M, Shahrokhi A, Azimpour G, Yadollahi A, Kocsis E, Toth-Bodrogi E & Kovács T, *Environ Sci Pollut Res*, 28 (2021) 41492.

14 Islami rad S Z, Mansuri R & Rezaei G H, *J Radiat Res Appl Sci,* 16 (2023) 100753.

15 Othman S Q, Ahmed A H & Mohammed S I, *Environ Monit Assess,* 195 (2023) 1.

16 Garba N N, Rabi'u N, Aliyu A S, Kankara U M, Vatsa A M, Isma'ila A & Bello S, *Heliyon*, 9 (2023) e15791

17 Khatun M A, Ferdous J & Haque M M, *J Environ Prot (Irvine,. Calif),* 9 (2018) 1034.

18 Amatullah S, Rahman R, Ferdous J, Siraz M M M, Uddin M, Mahal S F, Rahman R, Ferdous J, Siraz M M M & Uddin M, *Int J Environ Anal Chem,* (2021) 1.

19 Ravisankar R, Vanasundari K, Suganya M, Raghu Y, Rajalakshmi A, Chandrasekaran A, Sivakumar S, Chandramohan J, Vijayagopal P & Venkatraman B, *Appl Radiat Isot,* 85 (2014) 114.

20 Prakash M M, Kaliprasad C S & Narayana Y, *J Radiat Res Appl Sci*, 10 (2017) 128.

21 Shetty P K, Narayana Y & Rajashekara K M, *J Radioanal Nucl Chem,* 290 (2011) 159.

22 Lokesh N, Ramanand P, Kavasara V & Yerol M, *Acta Geophys,* (2022) 0123456789. https://doi.org/10.1007/s11600-022-00866-9.

23 Jagadeesha B G & Narayana Y, *Radiochemistry,* 59 (2017) 104.

24 Suresh S, Rangaswamy D R, Sannappa J, Dongre S, Srinivasa E & Rajesh S, *J Radioanal Nucl Chem,* 331 (2022) 1869.

25 Chandrasekaran V S A & Tamilarasi S M A, *J Radioanal Nucl Chem,* 331 (2022) 1495.

26 ICRP, *Recommendations of the International Commission on Radiological Protection,* 1991.

27 Lu X, Yang G & Ren C, *Radiat Phys Chem,* 81 (2012) 780.

28 Asaduzzaman K, Mannan F & Khandaker M U, Assessment of Natural Radioactivity Levels and Potential Radiological Risks of Common Building Materials Used in Bangladeshi Dwellings, (2015) 1.

29 Abdullahi S, Ismail A F & Samat S, *Nucl Eng Technol,* 51 (2019) 325.

30 Aladeniyi K, Arogunjo A M, Pereira A J S C, Khandaker M U, Bradley D A & Sulieman A, *Radiat Phys Chem*, 178 (2021) 109021.

31 El-taher A, Makhluf S, Nossair A & Halim A S A, *Appl Radiat Isot*, 68 (2010) 169.

32 Turhan Ş, Kurnaz A & Karataşlı M, *Environ Sci Pollut Res,* 29 (2022) 10575.

33 Senthilkumar G, Raghu Y, Sivakumar S, Chandrasekaran A, Anand D P, Ravisankar R, Raghu Y, Sivakumar S, Chandrasekaran A & Anand D P, *J Radiat Res Appl Sci*, 7 (2019) 116.

34 Ibrahim N, *J Environ Radioact,* 43 (1999) 255.

35 Tuo F, Peng X, Zhou Q, Zhang J, *Radiat Prot Dosimetry,* 188 (2020) 316.

36 Sharma B, Singh N, Devi P, Basu H, Saha S & Singhal R, *Radiat Prot Environ,* 40 (2017) 149.

37 Mohammed R S & Ahmed R S, *Environ Earth Sci,* 76 (2017) 1.

38 Monica S, Prasad V A, Soniya S & Jojo P, *Radiat Prot Environ,* 39 (2016) 38.

39 Raghu Y, Ravisankar R, Chandrasekaran A, Vijayagopal P & Venkatraman B, *J Taibah Univ Sci,* 11 (2017) 523.

40 Ravisankar R, Vanasundari K, Chandrasekaran A, Rajalakshmi A, Suganya M, Vijayagopal P & Meenakshisundaram V, *Appl Radiat Isot,* 70 (2012) 699.

41 Raghu Y, Chandrasekaran A & Ravisankar R, *Acta Ecol Sin*, (2020). https://doi.org/10.1016/j.chnaes.2019.12.006.

42 Tanasković I, Golobocanin D & Miljević N, *J Geochemical Explor*, 112 (2012) 226.

43 Asfahani J, *Appl Radiat Isot,* 145 (2019) 209.

44 Ramasamy V, Suresh G, Meenakshisundaram V & Ponnusamy V, *Appl Radiat Isot*, 69 (2011) 184.

45 Raghu Y, Ravisankar R, Chandrasekaran A, Vijayagopal P & Venkatraman B, *Health Phys,* 111 (2016) 265.

46 Hamideen M S, Bdair O M, Chandrasekaran A & Saleh H, *Int J Environ Anal Chem,* 100 (2020) 189.